

1 **Perforin-2 Permeabilizes the Envelope of Phagocytosed Bacteria**

2

3 Fangfang Bai, Ryan M. McCormack, Suzanne Hower, Gregory V. Plano, Mathias G. Lichtenheld,
4 George P. Munson*

5

6 Department of Microbiology and Immunology, Miller School of Medicine, University of Miami,
7 Miami, 33163 USA

8 *Correspondence: George P. Munson, gmunson@miami.edu

9 Running title: Perforin-2

10

11

12 **Abstract**

13 Perforin-2, the product of the *MPEG1* gene, limits the spread and dissemination of bacterial
14 pathogens in vivo. It is highly expressed in murine and human phagocytes, and macrophages
15 lacking Perforin-2 are compromised in their ability to kill phagocytosed bacteria. In this study we
16 used *Salmonella typhimurium* as a model intracellular pathogen to elucidate the mechanism of
17 Perforin-2's bactericidal activity. In vitro Perforin-2 was found to facilitate the degradation of
18 antigens contained within the envelope of phagocytosed bacteria. In contrast, degradation of a
19 representative surface antigen was found to be independent of Perforin-2. Consistent with our in
20 vitro results a protease sensitive, periplasmic superoxide dismutase (SodCII) contributed to the
21 virulence of *S. typhimurium* in Perforin-2 knockout but not wild-type mice. In aggregate our
22 studies indicate that Perforin-2 breaches the envelope of phagocytosed bacteria facilitating the
23 delivery of proteases and other antimicrobial effectors to sites within the bacterial envelope.

24

25

26 Introduction

27 Macrophages and neutrophils phagocytose microorganisms to remove them from blood and
28 tissues. As the phagosome matures the multisubunit NADPH oxidase assembles on its
29 membrane and reduces O₂ to generate superoxide in the lumen of the phagosome (Karimi et al.,
30 2014; Nauseef, 2004). The products of this respiratory burst –superoxide and subsequently other
31 reactive oxygen species (ROS)– are bactericidal. The destruction and degradation of
32 phagocytosed microbes is further facilitated by acidification of the phagosome and fusion with
33 lysosomes that deliver oxygen-independent antimicrobial effectors such as lysozyme,
34 glycosylases, proteases, and other hydrolases (Cederlund et al., 2011). Large antimicrobials such
35 as proteases and other hydrolases are typically membrane impermeable molecules. This property
36 is advantageous in that it allows them to be confined within lysosomes and phagolysosomes.
37 However it also precludes them from reaching the internal components of phagocytosed bacteria.
38 For example, lysozyme hydrolyzes β(1,4)-glycosidic bonds of peptidoglycan; the primary
39 structural component of bacterial cell walls. In gram-negative bacteria peptidoglycan resides in
40 the space between the outer and inner membranes; i.e., the periplasm. Thus, for these bacteria a
41 breach of the outer membrane must precede lysozyme-dependent degradation of peptidoglycan
42 (Ellison and Giehl, 1991; Martinez and Carroll, 1980). For hydrolases with targets in the cytosol of
43 gram-negative bacteria the challenge is two-fold as their substrates are bound by both an inner
44 and outer membrane.

45 Studies over the past two decades have shown that antimicrobial peptides such as the defensins
46 and cathelicidins attack and disrupt bacterial membranes (Gallo et al., 1997; Turner et al., 1998;
47 Wiesner and Vilcinskas, 2010; Zanetti, 2004). NMR studies of the cathelicidin LL-37 suggest that
48 the peptide destabilizes the bacterial membrane by carpeting rather than penetrating the lipid
49 bilayer (Henzler Wildman et al., 2003). Within phagolysosomes the murine cathelicidin CRAMP
50 has been shown to be active against phagocytosed *Salmonella*; most likely by disruption of the
51 bacterium's outer membrane (Kim et al., 2010; Rosenberger et al., 2004). Likewise, cathelicidin
52 LL-37 may play a similar role in human phagocytes (Sonawane et al., 2011; Stephan et al.,
53 2016). Nearly coincident with the initial descriptions of LL-37 and CRAMP the *Mpeg1* gene was
54 identified as a potential marker of mammalian macrophages due to its relatively high expression
55 in mature human and murine macrophages (Gallo et al., 1997; Gudmundsson et al., 1996;
56 Spilsbury et al., 1995). *Mpeg1* encodes a 73 kDa protein referred to as Perforin-2 and in their
57 initial report Spilsbury et al. noted its partial homology to the membrane attack complex perforin
58 (MACPF) domain of Perforin; the cytolytic protein of natural killer cells and cytotoxic T
59 lymphocytes (Spilsbury et al., 1995). Unlike the carpet mechanism of cathelicidins Perforin is a
60 large polypeptide that polymerizes on target membranes. A concerted structural transition results
61 in a pore through the lipid bilayer whose hydrophilic channel is lined with amphipathic β-strands
62 donated by the MACPF domains (Law et al., 2010; Voskoboinik et al., 2015). It is through this
63 channel, either at the cell surface as originally hypothesized or within endosomal membranes as
64 a more recent study suggest, that granzyme proteases enter tumor and virally infected cells to
65 facilitate their destruction and lysis (Lichtenheld et al., 1988; Podack et al., 1989; Thiery et al.,
66 2011). MACPF domains are also present in the terminal complement proteins which form pores
67 in the outer membranes of gram-negative bacteria through a similar mechanism of polymerization
68 and structural transition (Dudkina et al., 2016).

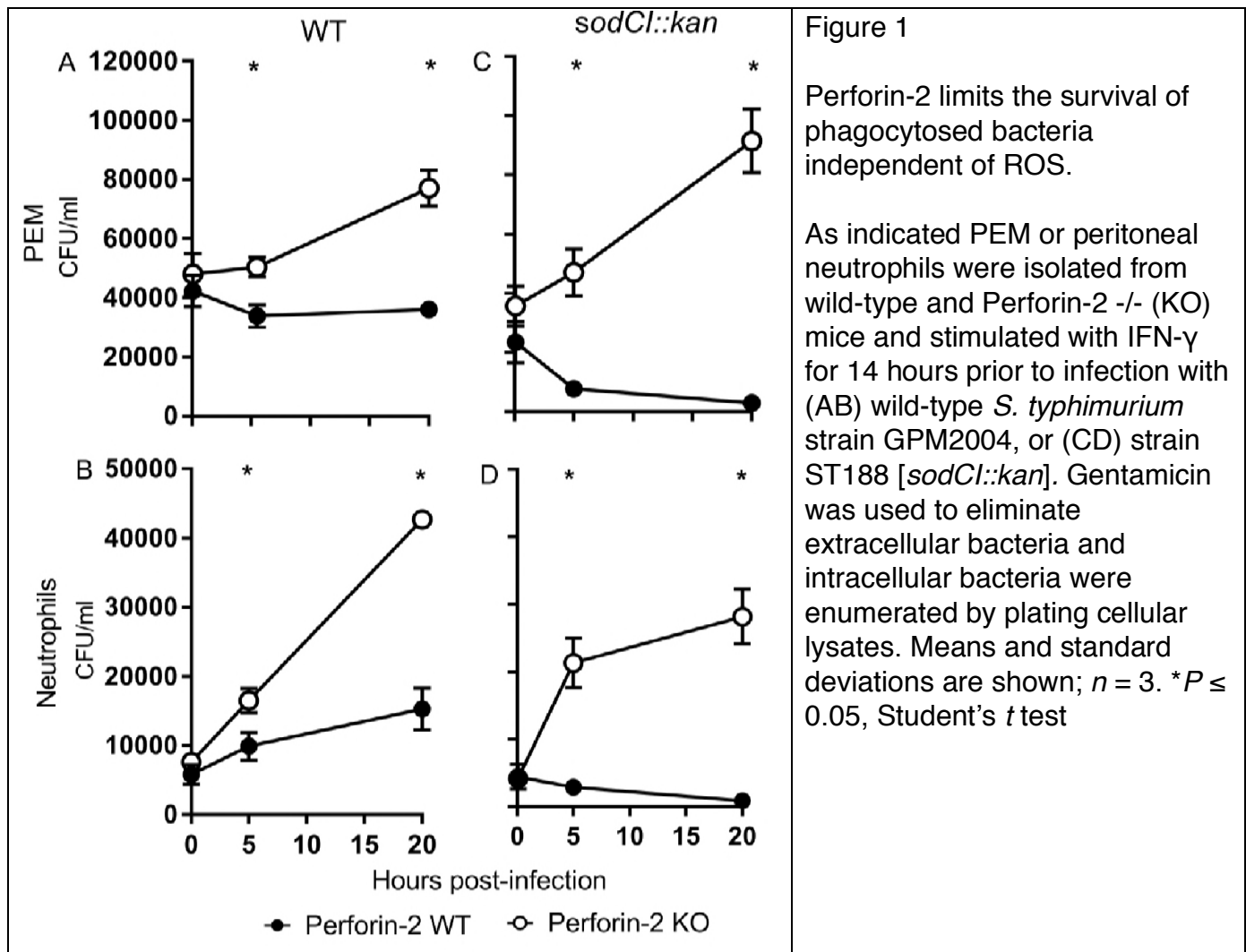
69 Despite the homology of mammalian Perforin-2 to known pore forming proteins there was no
70 further elaboration of its function until 2013; nearly two decades after the initial report of Spilsbury
71 et al. (McCormack et al., 2013; Spilsbury et al., 1995). In 2013 McCormack et al. demonstrated
72 that the expression of Perforin-2 correlated with the killing of phagocytosed gram-negative, -

73 positive, and acid-fast bacteria in vitro (McCormack et al., 2013). Subsequent studies with
74 transgenic mice found that Perforin-2 *-/-* mice are unable to limit the proliferation and
75 dissemination of infectious bacteria. Not surprisingly, Perforin-2 knockout mice succumb to
76 infectious doses that are non-lethal to their wild-type littermates (McCormack et al., 2016;
77 McCormack et al., 2015a; McCormack et al., 2015b). Moreover this defect is not limited to a
78 particular route of infection nor pathogen. Nor is it limited to mammalian Perforin-2 as similar
79 results have been reported with zebrafish as the model organism (Benard et al., 2015). In
80 aggregate these latter studies have demonstrated that Perforin-2 is associated with broad
81 spectrum bactericidal activity. In this study we utilized *Salmonella typhimurium* as a model
82 pathogen to elucidate the mechanism of Perforin-2 dependent killing of phagocytosed bacteria.

83 **Results**

84 **Perforin-2 limits the survival of phagocytosed bacteria independent of ROS.**

85 Because the interactions between *Salmonella* sp. and macrophages have been extensively
86 characterized, we chose to exploit the *Salmonella*/phagocyte paradigm to probe the mechanism
87 of Perforin-2 dependent killing of phagocytosed bacteria (Steele-Mortimer, 2008). Accordingly,
88 peritoneal exudate macrophages (PEMs) and neutrophils isolated from wild-type and Perforin-2 *-*
89 *-/-* mice were infected with *Salmonella enterica* serovar Typhimurium (hereafter *S. typhimurium*).
90 As expected from previous studies that have shown *Salmonella* survives within macrophages, the
91 intracellular load of bacteria either increased or remained constant in wild-type phagocytes
92 (Figure 1AB). However, Perforin-2 deficient phagocytes had significantly higher intracellular loads
93 of *S. typhimurium* than wild-type phagocytes (Figure 1AB). This demonstrates that Perforin-2
94 limits the survival and/or replication of phagocytosed *S. typhimurium* and is consistent with
95 previous studies that have shown Perforin-2 is a potent antimicrobial effector against *Salmonella*
96 as well as gram-positive and acid-fast bacteria (Fields et al., 2013; McCormack et al., 2016;
97 McCormack et al., 2015a; McCormack et al., 2015b).



98 One of the aforementioned studies also investigated the relationship between reactive oxygen
 99 species (ROS) and Perforin-2 and concluded that the bactericidal activity of ROS was dependent
 100 upon Perforin-2 (McCormack et al., 2015a). This was based on two principle findings. First,
 101 chemical inhibition of ROS production significantly enhanced the survival of phagocytosed *S.*
 102 *typhimurium* –relative to mock treated cells– in wild-type but not Perforin-2 deficient PEMs.
 103 Second, wild-type PEMs killed a Δ *sodCl* strain of *S. typhimurium* much more efficiently than wild-
 104 type *S. typhimurium*. SodCl is a periplasmic superoxide dismutase that neutralizes ROS and thus
 105 promotes the survival of *S. typhimurium* within phagosomes (Krishnakumar et al., 2004;
 106 McCormack et al., 2015a). However, the *sodCl* mutant was found to be no less fit than the wild-
 107 type strain when Perforin-2 $-/-$ PEMs were used. Thus, both a chemical and genetic analysis
 108 suggest that ROS is not a significant bactericidal effector when Perforin-2 is absent.

109 As with the previous study we observed similar effects with both PEMs and neutrophils. In either
 110 case the *S. typhimurium sodCl* mutant was efficiently killed by Perforin-2 proficient but not
 111 deficient phagocytes (Figure 1CD). The source of phagocytic ROS is the multisubunit NADPH
 112 oxidase NOX2 (Panday et al., 2015). Assembly of the enzymatic complex involves the
 113 translocation of cytosolic proteins to the endosomal membrane to form the active complex that
 114 generates the respiratory burst (Panday et al., 2015). Likewise Perforin-2, a transmembrane
 115 protein of cytosolic vesicles, dynamically translocates to and fuses with phagocytic vesicles
 116 containing bacteria (McCormack et al., 2015a; McCormack et al., 2015b). This raised the
 117 possibility that Perforin-2 is involved in the assembly and/or activation of the NADPH oxidase. If

118 true the respiratory burst would be deficient in Perforin-2 *-/-* phagocytes and would account for
119 the survival of *S. typhimurium sodCI* mutants in Perforin-2 deficient phagocytes.

120 To determine whether or not Perforin-2 is required for ROS production a luminol based
121 chemiluminescence assay was used to quantify ROS productions in IFN- γ primed PEMs,
122 peritoneal macrophages isolated without thioglycollate stimulation, and neutrophils from wild-type
123 and Perforin-2 knockout mice. We found that ROS production was equally robust in wild-type and
124 Perforin-2 *-/-* macrophages that were stimulated with PMA or LPS (Figure 2AB). The kinetics of
125 ROS production was also similar as macrophages of both genotypes exhibited peak ROS
126 production at 60 min. To confirm that the chemiluminescent signal was due to ROS production by
127 a NADPH oxidase, phagocytes were pretreated with diphenyleneiodonium chloride (DPI); an
128 inhibitor of NADPH oxidases. As expected DPI treated cells produced negligible amounts of ROS
129 (Figure 2). Likewise, ROS production was also negligible in unstimulated macrophages (data not
130 shown). As with macrophages, we found few statistically significant differences between ROS
131 production in wild-type and Perforin-2 *-/-* neutrophils (Figure 2CD). Thus, we conclude that
132 impaired ROS production cannot account for the survival of *S. typhimurium $\Delta sodCI$* mutants in
133 Perforin-2 *-/-* phagocytes.

134

135

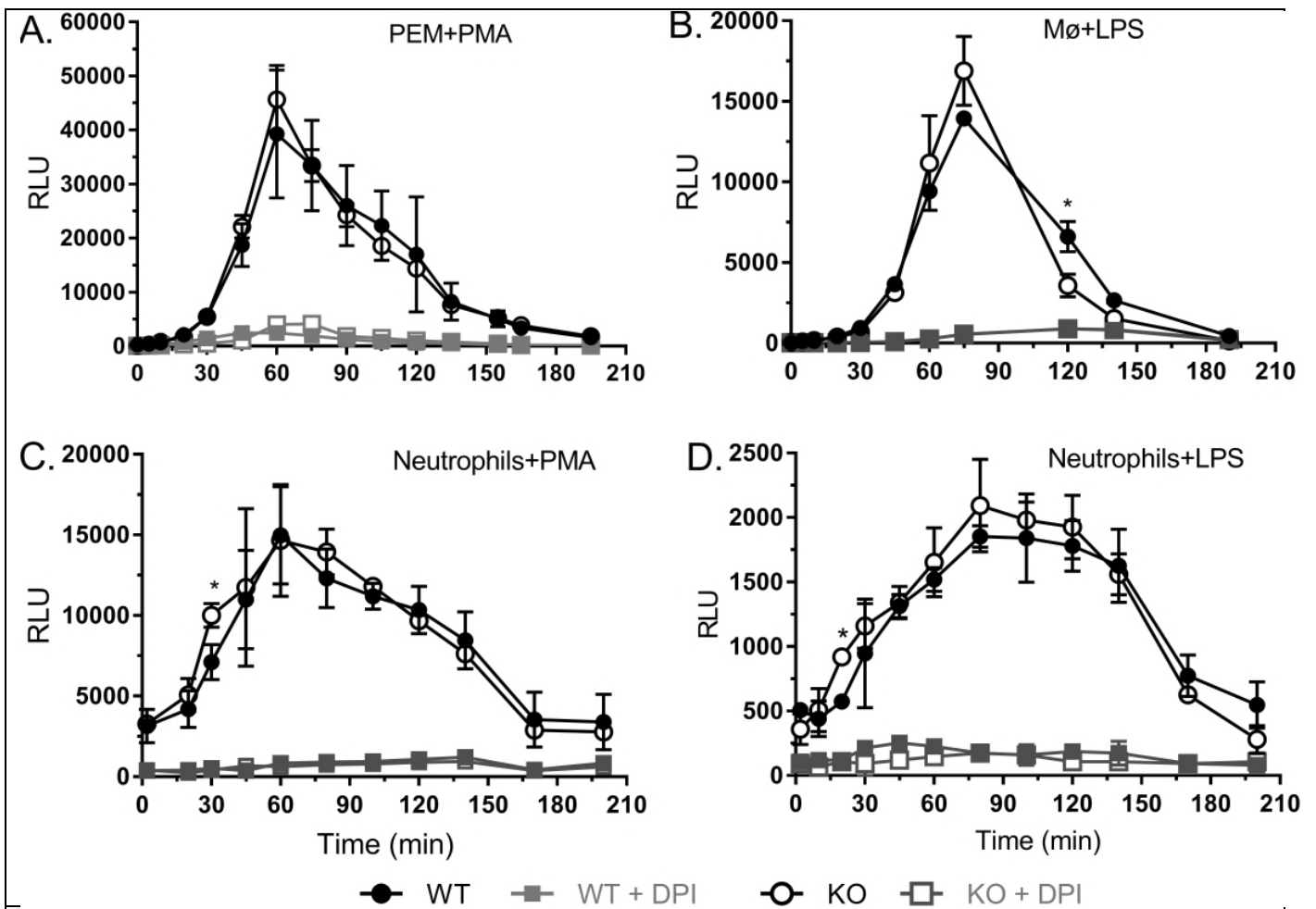


Figure 2

Perforin-2 is not required for ROS production in phagocytes.

As indicated wild-type and Perforin-2 $-/-$ (KO) peritoneal (A,B) macrophages and (C,D) neutrophils were stimulated with PMA or LPS to elicit ROS production which was detected by luminal based chemiluminescence. An enhancer was added to amplify chemiluminescence when macrophages were used. As indicated some cells were also treated with DPI, an inhibitor of the phagocytic NADPH oxidase. ROS activity is reported as mean relative light units (RLUs) \pm SD; $n = 3$. * $P \leq 0.05$, Student's t test.

136

SodCI and SodCII are functionally redundant in Perforin-2 $-/-$ phagocytes.

137

138

139

140

141

142

143

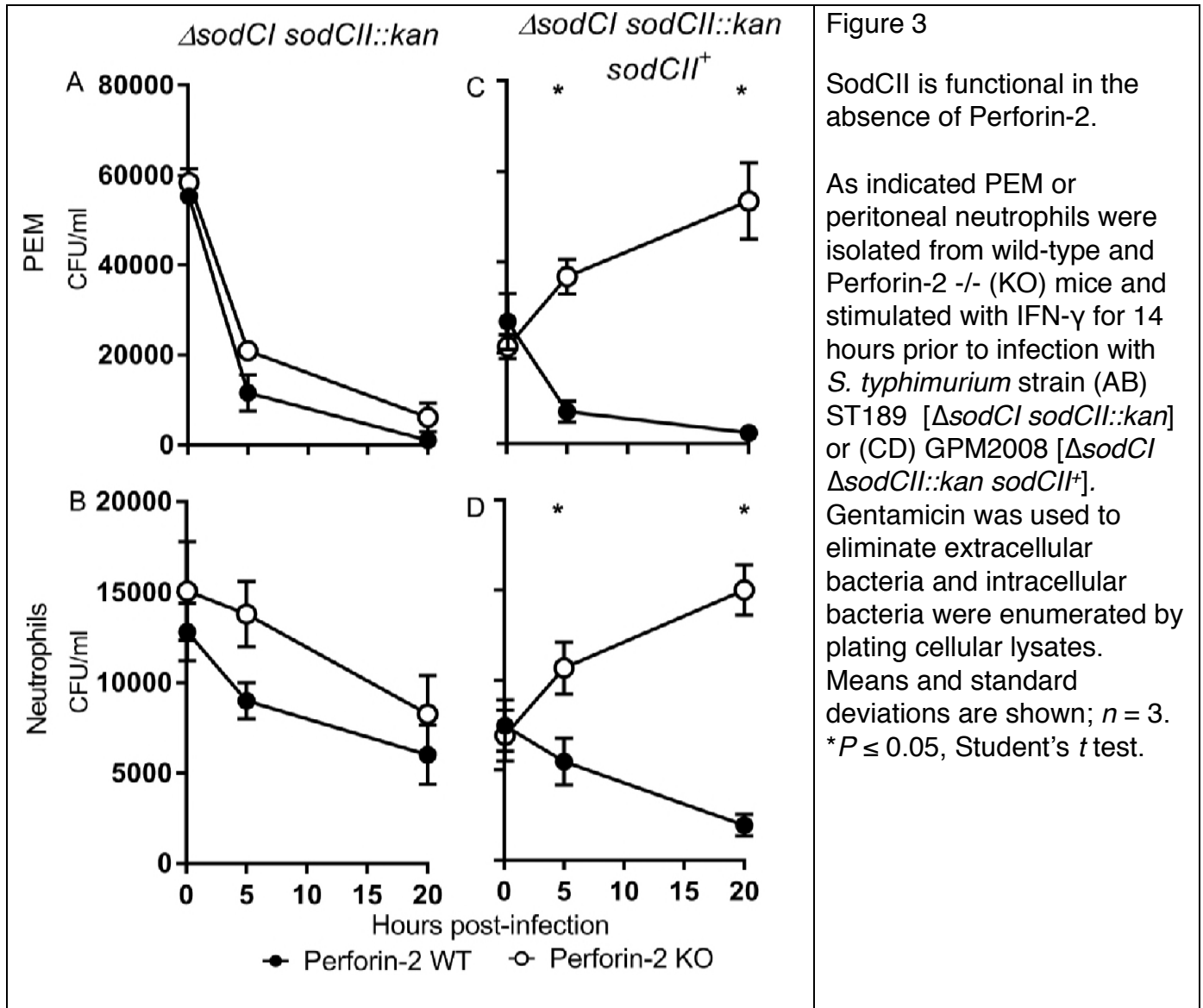
144

145

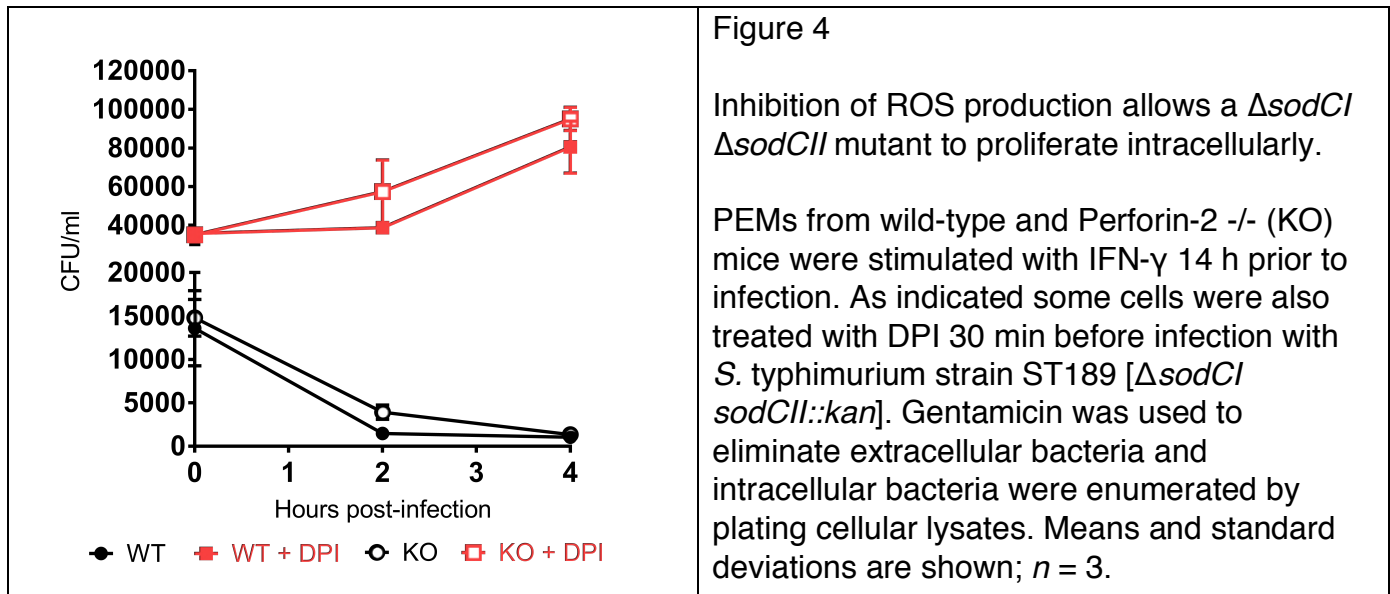
146

Having excluded the possibility that Perforin-2 deficiency results in impaired ROS production, we next considered the possibility that *S. typhimurium sodCI* mutants are resistant to ROS in Perforin-2 deficient but not proficient phagocytes. As the genome of *S. typhimurium* encodes a second periplasmic superoxide dismutase (SodCII) we considered the possibility that it provides resistance to ROS in Perforin-2 $-/-$ phagocytes even though previous studies have concluded that SodCII does not attenuate ROS toxicity in wild-type cells and animals (Kim et al., 2010; Krishnakumar et al., 2004). To determine whether or not SodCI and SodCII are functionally redundant we infected Perforin-2 proficient and deficient phagocytes with a *sodCI sodCII* double mutant. Unlike the $\Delta sodCI sodCII^+$ strain which was killed by wild-type but not Perforin-2 knockout phagocytes (Figure 1CD), the $\Delta sodCI sodCII::kan$ strain was killed by both Perforin-2 $+/+$ and $-/-$

147 phagocytes (Figure 3AB). Moreover, treatment with the NADPH oxidase inhibitor DPI
 148 demonstrated that killing of the double mutant was ROS dependent in both Perforin-2 +/+ and -/-
 149 PEMs (Figure 4). Complementation of the double mutant with *sodCII* allowed the complemented
 150 strain to proliferate in Perforin-2 -/- but not wild-type phagocytes (Figure 3CD). Thus, in
 151 agreement with previous studies we conclude that SodCII does not protect against ROS in wild-
 152 type phagocytes. However, the nullification of SodCII is clearly dependent upon Perforin-2
 153 because SodCII is able to protect phagocytosed *S. typhimurium* from the bactericidal effects of
 154 ROS in Perforin-2 -/- phagocytes.



155



156

157 Perforin-2 facilitates the degradation of antigens enclosed within the bacterial envelope.

158 Although SodCI and SodCII have similar enzymatic properties, only SodCI provides resistance to
159 endosomal ROS in wild-type phagocytes (Krishnakumar et al., 2004). Studies by the Slauch
160 laboratory have shown that this phenomenon is not the result of differential expression
161 (Krishnakumar et al., 2004). Rather it is due to differential degradation of the two superoxide
162 dismutases; SodCI is protease resistant while SodCII is protease sensitive (Kim et al., 2010;
163 Krishnakumar et al., 2004; Krishnakumar et al., 2007). Thus, SodCII does not protect
164 phagocytosed *S. typhimurium* because it is proteolytically degraded. However SodCII is
165 functional in Perforin-2 $-/-$ phagocytes (Figure 3). Therefore, we considered it possible that the
166 degradation of SodCII is Perforin-2 dependent. To determine whether or not this is the case we
167 infected wild-type and knockout PEMs with a strain of *S. typhimurium* expressing SodCII-FLAG
168 so that we could track the persistence of SodCII in the periplasm with a monoclonal antibody
169 against the FLAG epitope. We also used antibodies against DnaK and flagellin to monitor the
170 abundance of cytoplasmic and surface antigens respectively. Western blots of intracellular
171 bacteria recovered 18 hours after infection revealed that extracellular flagellin, which was
172 abundant on the surface of the bacteria prior to phagocytosis, was efficiently degraded in both
173 wild-type and knockout PEMs (Figure 5A). In contrast there was a clear difference in the
174 abundance of SodCII in bacteria recovered from Perforin-2 $-/-$ and $+/+$ PEMs (Figure 5A). This
175 was not due to differences in bacterial load because the difference in SodCII abundance was
176 statistically significant when experimental replicates were quantified and normalized to DnaK of
177 the bacterial cytoplasm (Figure 5B). A further indication that the bacterial loads were similar in
178 these experiments is the fact that the difference in the amount of DnaK normalized to host β -actin
179 was insignificant while the difference in the amount of SodCII normalized to β -actin was
180 significant (Figure 5B).

181 We also examined the degradation of the three bacterial antigens at earlier time points. Because
182 these experiments required significantly more phagocytes we used BMDM which can be obtained
183 at higher yields than PEMs. As with PEMs extracellular flagellin was efficiently degraded in both
184 wild-type and Perforin-2 $-/-$ BMDM (Figure 5C). There was also apparent degradation of both
185 SodCII and DnaK in both types of cells. Nevertheless there was less SodCII in bacteria recovered
186 from wild-type than knockout phagocytes. This difference was statistically significant at 3 and 6
187 hours when normalized to DnaK even though concurrent degradation of DnaK likely results in an

188 underestimation of the difference (Figure 5D). The degradation of DnaK also appears to lag that
189 of SodCII; although, it is unclear if this is due to differences in protease accessibility and/or
190 susceptibility. Differences in expression may also contribute to the apparent differences in
191 degradation rates of SodCII compared to DnaK. Relative to β -actin the differences in SodCII in
192 wild-type compared to Perforin-2 $-/-$ BMDM was significant even at the 1 hour time point. This
193 cannot be due to higher loads of the bacteria in Perforin-2 $-/-$ phagocytes because the amount of
194 DnaK normalized to β -actin also decreased over time; even in knockout cells. Additionally,
195 extrapolation of our PEM bactericidal assays suggest the differences in bacterial loads is likely to
196 be negligible at early time points; especially, at 1 hour. In aggregate these results demonstrate
197 that Perforin-2 facilitates the degradation of internal –but not extracellular– antigens of
198 phagocytosed bacteria.

199

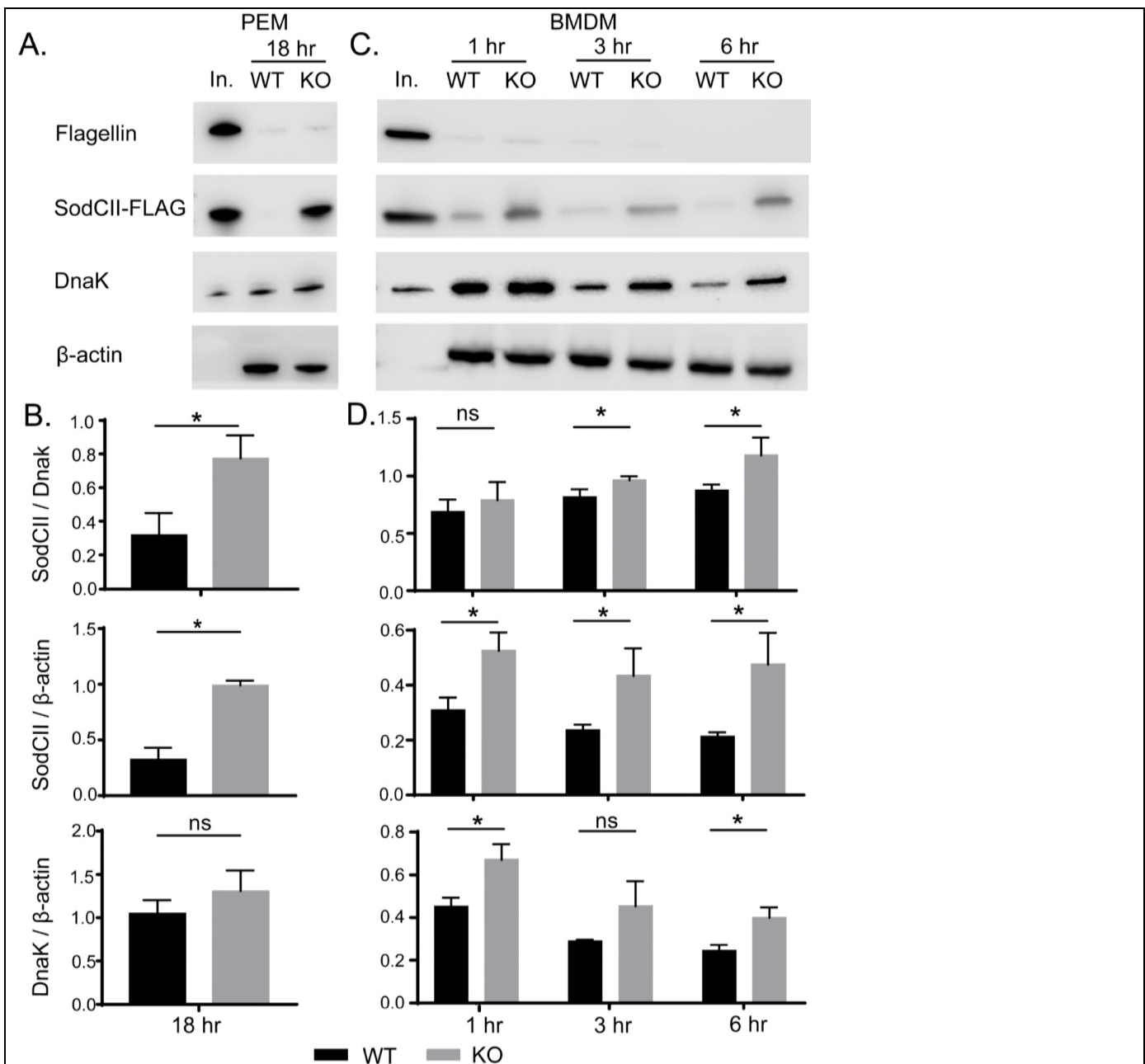


Figure 5

Perforin-2 facilitates the degradation of antigens enclosed within the bacterial envelope.

(A) PEMs isolated from Perforin-2 $+/+$ and $-/-$ (KO) mice were infected with a strain of *S. typhimurium* expressing SodCII-FLAG. After 18 hours the phagocytosed bacteria were recovered and the indicated antigens were detected by Western blot.

(B) Quantification of Western blot data from three separate experiments in PEMs

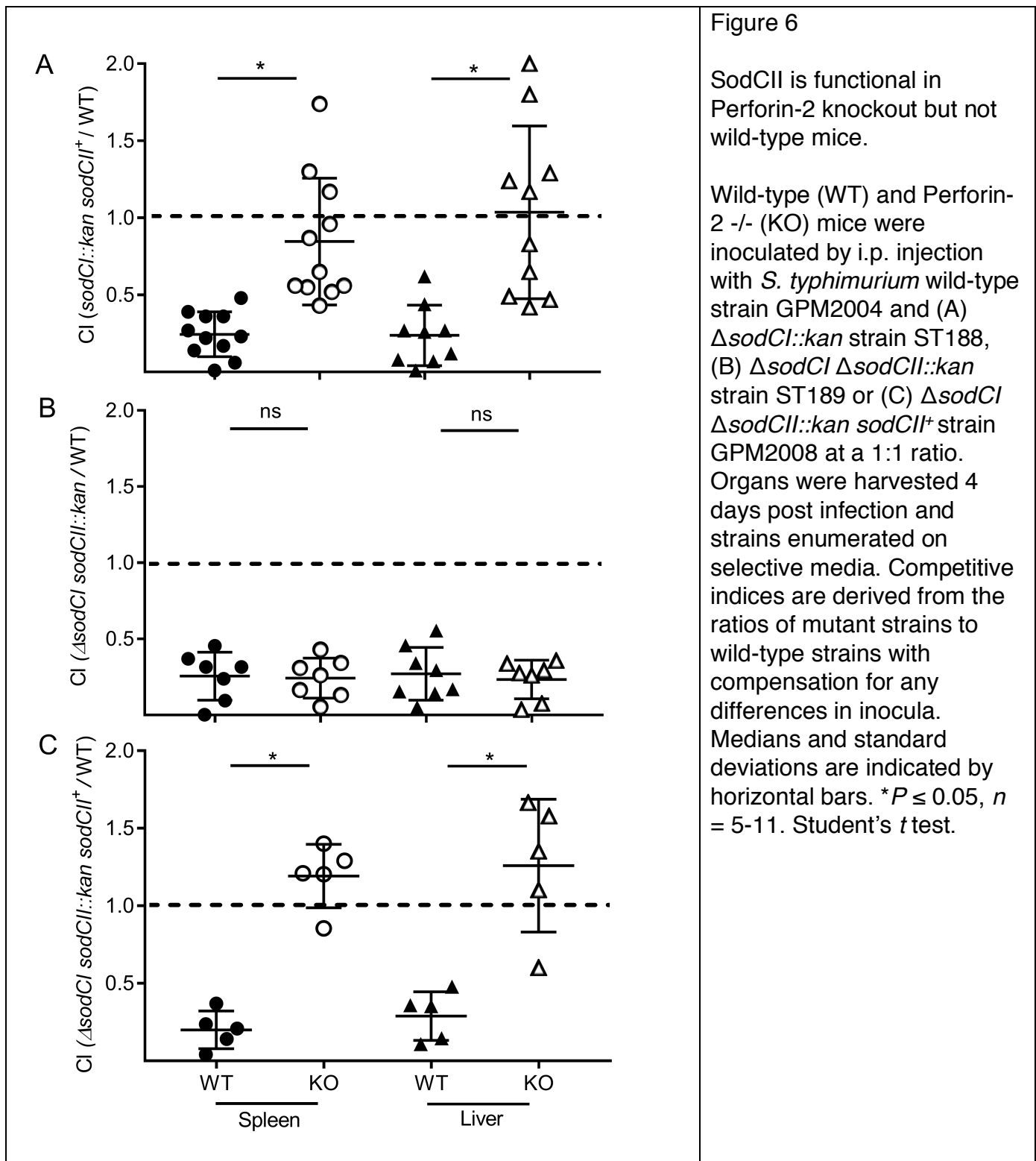
(C) Similar infection experiments were conducted with BMDMs except the phagocytosed bacteria were recovered at 1, 3, and 6 hours post phagocytosis.

(D) Quantification of Western blot data from three separate experiments in BMDMs. Means and standard deviations are shown; $n = 3$. * $P \leq 0.05$, Student's t test.

Abbreviations: In., inoculum; ns, not significant

202 **Perforin-2 negates SodCII in vivo.** Having established that Perforin-2 facilitates the degradation
203 of SodCII in vitro, the relevance of our observations were evaluated in a murine infection model.
204 In brief, wild-type and Perforin-2 *-/-* mice were inoculated intraperitoneally with a mixture of wild-
205 type *S. typhimurium* and a *sodCI* mutant at a 1:1 ratio. Four days after infection liver and spleen
206 homogenates were plated on selective media to enumerate the load of each strain. Consistent
207 with previous studies fewer *sodCI::kan* bacteria were recovered than wild-type bacteria recovered
208 from Perforin-2 *+/+* mice. The derived competitive indices were accordingly low and demonstrate
209 that the *sodCI* mutant is significantly attenuated in Perforin-2 proficient mice (Figure 6A). In
210 contrast, there was little to no attenuation of the *sodCI::kan* strain in Perforin-2 *-/-* mice as
211 indicated by competitive indices near or at 1.0 (Figure 6A). Similar results were obtained with a
212 strain of *S. typhimurium* that had spontaneously lost the pSLT virulence plasmid (Figure S1)
213 (McClelland et al., 2001). Thus, SodCI is not essential in the absence of Perforin-2.

214 Based on our in vitro studies the persistence of SodCII was the most likely explanation for the
215 lack of attenuation of the *sodCI* mutant in Perforin-2 knockout mice. Indeed this was found to be
216 the case because a *sodCI sodCII* double mutant was found to be significantly attenuated relative
217 to wild-type bacteria in Perforin-2 *-/-* mice (Figure 6B). Furthermore, complementation of the
218 *sodCI sodCII* double mutant with *sodCII* resulted in a strain that was as virulent as wild-type *S.*
219 *typhimurium* in Perforin-2 *-/-* mice (Figure 6C). In fact there appeared to be a slight competitive
220 advantage of the complemented strain over the wild-type strain as indicated by competitive
221 indices > 1. This could be the result of higher expression levels of *sodCII* from a heterologous
222 promoter in our construct. In contrast, complementation with *sodCII* failed to rescue the double
223 mutant in wild-type mice (Figure 6C). In aggregate the in vivo studies demonstrate that SodCII
224 confers a protective advantage in Perforin-2 *-/-* but not wild-type mice. As such they are
225 consistent with our in vitro finding that Perforin-2 facilitates the degradation of SodCII.



226

227 Discussion

228 Perforin-2 is a type I transmembrane protein that we have previously shown localizes to
 229 endosomal vesicles as well as the endoplasmic reticulum, Golgi, and plasma membrane
 230 (McCormack et al., 2015a). A separate study that focused on the proteome of endocytic vesicles
 231 also found that Perforin-2 is present in endosomes following phagocytosis of latex beads by J774

232 macrophages (Duclos et al., 2011). The same study also found that Perforin-2 was more
233 abundant in late endosomes and lysosomes than early endosomes. Perforin-2 is also coincident
234 with subunits of the phagocytic NAPDH oxidase, proton transporters, and many other
235 antimicrobial effectors of phagosomes and/or the phagolysosomes (Duclos et al., 2011;
236 Nakamura et al., 2014). LPS stimulation of BMDM has also been shown to increase the
237 abundance of Perforin-2 in endolysosomes compared to untreated cells (Nakamura et al., 2014).
238 This is consistent with our own studies in which we reported that LPS results in the accumulation
239 of Perforin-2 in vesicular structures and that Perforin-2 colocalizes with phagocytosed bacteria
240 such as *Escherichia coli* and *S. typhimurium* (McCormack et al., 2015a; McCormack et al.,
241 2015b). In aggregate these studies demonstrate that the subcellular distribution of Perforin-2 is
242 consistent with its ability to facilitate the destruction of phagocytosed bacteria.

243 Although most phagocytosed bacteria are rapidly killed some are able to resist phagocytic
244 antimicrobials and even survive within professional phagocytes. The latter includes *S.*
245 *typhimurium* which must survive the respiratory burst and other antimicrobial assaults prior to the
246 formation of *Salmonella* containing vacuoles; specialized niches within macrophages that afford
247 the pathogen a more favorable environment than phagosomes or phagolysosomes (Anderson
248 and Kendall, 2017). A central player in the survival of the respiratory burst is SodCI; a periplasmic
249 superoxide dismutase that converts superoxide to hydrogen peroxide which is subsequently
250 detoxified by bacterial catalases and peroxidases (Aussel et al., 2011; Hebrard et al., 2009;
251 Slauch, 2011; Storz and Imlay, 1999). The pivotal role of SodCI in protecting *Salmonella* from
252 ROS has been confirmed by several studies that have shown that *sodCI* mutants are more
253 susceptible to ROS killing in vitro and less virulent than wild-type *Salmonella* in vivo (Craig and
254 Slauch, 2009; Fang et al., 1999; Krishnakumar et al., 2004; Krishnakumar et al., 2007). However
255 we have found that a *sodCI* null mutant is able to proliferate in Perforin-2 deficient phagocytes.
256 Moreover the *sodCI* null mutant is as virulent as wild-type *S. typhimurium* in Perforin-2 deficient –
257 but not proficient– mice. Because we have found that the production of phagocytic ROS is
258 independent of Perforin-2, the survival of the *sodCI* mutant is not due to differences in ROS
259 production. Rather it is due to the persistence of SodCII, a second periplasmic superoxide
260 dismutase, in Perforin-2 deficient phagocytes. Consistent with our in vitro results we have also
261 found that SodCI and SodCII are functionally redundant in Perforin-2 knockout mice.

262 The persistence of SodCII was unexpected because previous studies have shown that it is
263 normally degraded by proteases of the phagolysosome (Krishnakumar et al., 2004; Krishnakumar
264 et al., 2007). In contrast SodCI is resistant to proteolytic degradation and thus provides resistance
265 to ROS in the phagolysosome (Krishnakumar et al., 2004). Our results in Perforin-2 +/+ cells and
266 animals are consistent with these latter studies because *sodCII* is unable to complement a *sodCI*/
267 *sodCII* double mutant. However, *sodCII* is able to complement the double mutant in Perforin-2 -/-
268 animals and isolated phagocytes. Thus, the presence of Perforin-2 is associated with the
269 inactivation of SodCII.

270 How does Perforin-2 inactivate SodCII? Consistent with previous studies we have shown that
271 SodCII is proteolytically degraded in the phagosome and/or phagolysosome in Perforin-2
272 proficient cells (Krishnakumar et al., 2004; Krishnakumar et al., 2007). However, the degradation
273 of SodCII is significantly attenuated in phagocytes lacking Perforin-2. Similar results were
274 observed with cytoplasmic DnaK in BMDM. This was not due to a general defect in protease
275 activity in the phagolysosome because the surface antigen flagellin was degraded whether or not
276 Perforin-2 was present. Thus, Perforin-2 facilitates the degradation of antigens contained within
277 the envelope of phagocytosed bacteria. However, it is unlikely that Perforin-2 is itself a protease
278 because it lacks significant homology to a known protease or protease motif. What Perforin-2

279 does have is a MACPF domain (Figure 7) (McCormack and Podack, 2015; Ni and Gilbert, 2017;
280 Podack and Munson, 2016). This suggest that Perforin-2 is a pore forming protein and putative
281 Perforin-2 pores have been imaged by transmission electron microscopy (McCormack et al.,
282 2015a). However to date it has not been possible to confirm that the imaged structures contain
283 Perforin-2 due to the absence of suitable antibodies. Nor has it been confirmed that the structures
284 are in fact pores. However, other MACPF containing proteins such as complement protein C9
285 and Perforin have been shown to polymerize and form pores in lipid membranes (Dudkina et al.,
286 2016; Law et al., 2010; Podack et al., 1989; Podack et al., 1982; Podack and Tschopp, 1982). For
287 example, 22 monomers of C9 polymerize to form a pore in the outer membrane of gram-negative
288 bacteria with an inner diameter of 120 Å (Dudkina et al., 2016; Podack et al., 1982; Tschopp and
289 Podack, 1981). Because Perforin-2 is a type I transmembrane protein with its membrane
290 spanning alpha helix near its carboxy-terminus, the MACPF domain of Perforin-2 would reside in
291 the lumen of endosomes and phagosomes. In this orientation its MACPF domain would reside in
292 the same compartment as phagocytosed bacteria. Thus, we propose that Perforin-2 polymerizes
293 – perhaps after cleavage from its transmembrane domain by a lysosomal protease– and forms
294 pores in the envelope of phagocytosed bacteria (Figure 7). This model is consistent with our
295 experimental observations with *S. typhimurium* since the protease that degrades SodCII would
296 enter the periplasmic space through poly-Perforin-2 pores. Because SodCII is not anchored in the
297 periplasm, it may also diffuse through the pore and be degraded in the lumen of the phagosome
298 (Kim et al., 2010; Krishnakumar et al., 2004; Krishnakumar et al., 2007). In either case SodCII is
299 able to persist in the periplasm and protect the bacterium from the bactericidal effects of ROS
300 when Perforin-2 is absent.

301 In addition to Perforin-2 there is evidence that the cathelicidins CRAMP and LL-37 also play a
302 role in disrupting the envelope of phagocytosed gram-negative bacteria in murine and human
303 macrophages respectively (Kim et al., 2010; Rosenberger et al., 2004; Sonawane et al., 2011;
304 Stephan et al., 2016). Of particular relevance to this study are previous studies that have shown
305 that CRAMP is active against phagocytosed *S. typhimurium* (Kim et al., 2010; Rosenberger et al.,
306 2004). In one it was shown that CRAMP inhibits the division of *S. typhimurium*. The result was
307 filamentous bacteria and it was further shown that filamentation was protease dependent
308 (Rosenberger et al., 2004). In another study it was shown that CRAMP is associated with the loss
309 of SodCII from the periplasm of *S. typhimurium* in vitro (Kim et al., 2010). Moreover SodCII
310 promoted the survival of *S. typhimurium* in CRAMP deficient but not proficient mice. However in
311 the latter study the authors also noted that the loss of CRAMP failed to fully abolish the
312 degradation of SodCII. Our study suggest that this is most likely due to the activity of Perforin-2.
313 Although it is clear that Perforin-2 and cathelicidins can act independently of one another, it
314 remains to be determined if they also act synergistically. In the case of gram-negative bacteria a
315 particularly intriguing model is the possibility that Perforin-2 forms a conduit in the outer
316 membrane through which cathelicidin or other antimicrobial peptides transit to reach the bacterial
317 inner membrane. Alternatively the deployment of independent mechanisms to disrupt the
318 envelope of phagocytosed bacteria may be an insurance strategy against pathogen resistance to
319 any particular mechanism.

320

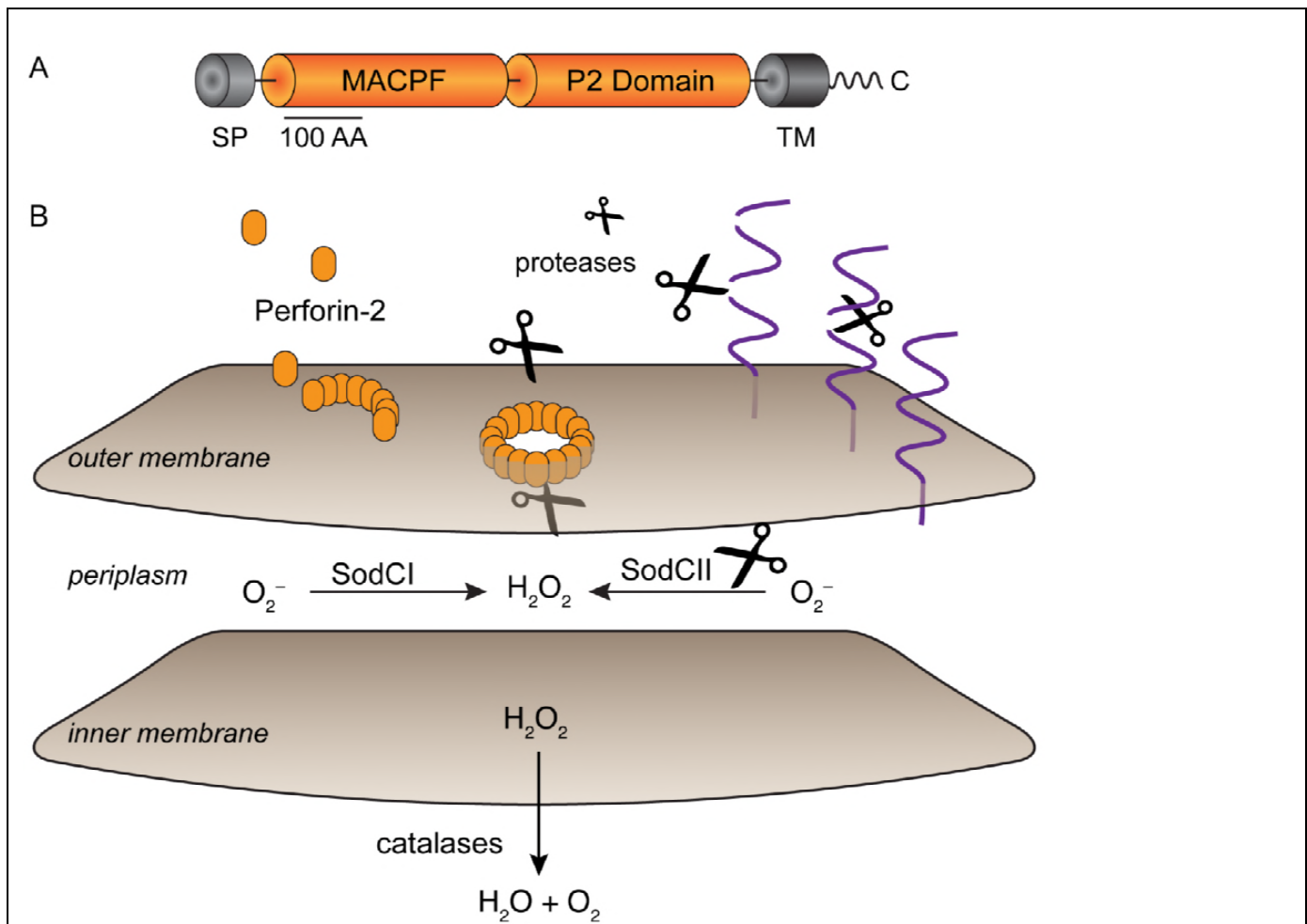


Figure 7

Model for Perforin-2 dependent degradation of SodCII.

(A) Domain organization of Perforin-2. MACPF domains are present in other proteins of the innate immune system and in the case of complement protein C9 and Perforin-1 have been shown to polymerize and form pores in lipid membranes. The P2 domain is a domain of unknown function that is conserved in orthologs of Perforin-2. As a type I transmembrane protein the MACPF domain of Perforin-2 would reside within the lumen of endosomes.

(B) Upon activation and likely cleavage from its transmembrane domain Perforin-2 polymerizes on the outer membrane of *S. typhimurium*. Subsequent pore formation allows proteases –and other antimicrobial effectors– to enter the periplasmic space and degrade SodCII. Alternatively, SodCII may diffuse through the poly-Perforin-2 pore and be destroyed in the lumen of the phagolysosome. Pores do not lead to the inactivation of SodCI because it is protease resistant and tethered within the periplasm. Abbreviations; SP, signal peptide; TM, transmembrane domain

321

322 Material And Methods

323 Mice. Perforin-2 $-/-$ 129X1/SvJ mice were produced at the University of Miami Miller School of
 324 Medicine Transgenic Core Facility as previously described (McCormack et al., 2015b). Wild-type
 325 129X1/SvJ and Perforin-2 $-/-$ mice of either sex were used at 2 to 6 months of age. Mice received

326 food and water *ad libitum* and were housed at an ambient temperature of 23°C on a 12 h
327 light/dark cycle under specific pathogen-free conditions. Mice were euthanized by CO₂ inhalation
328 followed by cervical dislocation. All procedures with animals were reviewed and approved by the
329 University of Miami's Institutional Animal Care and Use Committee.

330 Strains and Plasmids. Bacterial strains are listed in Table 1. Primer sequences are listed in Table
331 2. Strains constructed for this study are isogenic derivatives of *S. typhimurium* strain LT2 (Nikaido
332 et al., 1967). Plasmid pKD4 (Datsenko and Wanner, 2000) was used in PCR with primer pairs
333 *sodCI*-P1/*sodCI*-P2 or *sodCII*-P1/*sodCII*-P2 to generate kanamycin resistance cassettes
334 bracketed by recognition sites for FLP recombinase and flanking sequences targeting *sodCI* or
335 *sodCII*. Deletions of *sodCI* or *sodCII* were generated by λ Red-mediated recombination of the
336 cassettes into LT2 as described (Datsenko and Wanner, 2000). Recombinants were selected on
337 LB agar plates with kanamycin. Recombination sites were verified by PCR with flanking primer
338 pairs *sodCI*-MfeI/*sodCI*-HindIII for *sodCI::kan* and *sodCII*-EcoRI/*sodCII*-HindIII for *sodCII::kan*.
339 For the construction of double deletions FLP recombinase was used to excise the first cassette
340 prior to insertion of the second.

341 The *sodCII* gene was cloned from LT2 by PCR with primers *sodCII*-1238/*sodCII*-1239. The PCR
342 product was digested with XbaI and BamHI then ligated into the same sites of pAH63Tc, a
343 derivative of pAH63 (Haldimann and Wanner, 2001) in which the kanamycin resistance gene was
344 replaced with one conferring resistance to tetracycline. To complement *sodCII* mutants the
345 resulting plasmid, pAH63Tc-*sodCII*, was integrated into *attB_λ* of relevant strains by a site specific
346 recombinase as previously described (Haldimann and Wanner, 2001). The chloramphenicol
347 resistant strain GPM2004 was constructed by integration of pCAH63 (Haldimann and Wanner,
348 2001) into *attB_λ* of LT2. Plasmid pTrc99a*SodCII*3flag was constructed by HiFi DNA assembly
349 (New England Biolabs) of three PCR products: one carrying *sodCII* amplified from pAH63Tc-
350 *sodCII* with primers *sodCII*-1329/*sodCII*-1330, another carrying a triple FLAG epitope amplified
351 from pSUB11 (Uzzau et al., 2001) with primers 3flag-1331/3flag-1332, and the vector backbone
352 amplified from pTrc99a (Amann et al., 1988) with primers pTrc99a-1333/pTrc99a-1334. Bacteria
353 were cultured in Luria-Bertani (LB) broth or plates. As appropriate antibiotics were used at the
354 following concentrations: chloramphenicol, 10 μ g/ml; ampicillin, 100 μ g/ml; kanamycin, 50 μ g/ml;
355 tetracycline 7.5 μ g/ml.

356 Cell preparation. Peritoneal exudate macrophages (PEMs) were isolated as previously described
357 (Zhang et al., 2008). Briefly, mice were injected intraperitoneally with 1 ml of 4% Brewer
358 thioglycollate medium and peritoneal exudates were recovered after 4 days. A modified schedule
359 was used to collect PEM for ROS assays (Nathan and Root, 1977). In brief, mice were inoculated
360 on days 1 and 7, and exudates were collected on day 14. Resting macrophages were collected
361 from the peritoneal cavities of untreated mice. Peritoneal neutrophils were elicited and recovered
362 as previously described (Luo and Dorf, 2001). Briefly mice were injected intraperitoneally with 1
363 ml 9 % casein in PBS (2.7 mM KCl, 4.3 mM Na₂HPO₄, 1.47 mM KH₂PO₄, 137 mM NaCl, pH 7.4)
364 containing 0.9 mM CaCl₂ and 0.5 mM MgCl₂. A second injection was administered 16 h after the
365 first and exudates collected 3 h later. Cells were maintained in IMDM (Gibco) supplemented with
366 10 % fetal bovine serum (FBS) (Gibco) at 37°C in 5% CO₂. Bone marrow derived macrophage
367 (BMDM) were isolated from the femurs from the Perforin-2 WT and KO mice. The cells were
368 cultured in IMDM medium supplemented with 10% FBS, 20% L929 conditioned medium, and 10
369 mM L-glutamine. BMDM were cultured for 6 days before use, and the culture medium was
370 changed every 2 days.

371 Intracellular killing assays. Intracellular gentamicin protection assays were performed as
372 previously described (Laroux et al., 2005; Lutwyche et al., 1998; McCormack et al., 2013). Briefly,

373 3×10^5 PEM were seeded in 24 well plates in IMDM, 10 % FBS and incubated at 37°C in 5%
374 CO₂. Murine IFN-γ was added 14 hours before infection at a final concentration of 50 ng/ml.
375 Overnight cultures of bacteria were diluted 33 fold in LB and cultured aerobically at 37°C for 3
376 hours to mid-log at which point the optical absorbance of the culture at 600nm was ca. 0.6.
377 Bacteria were added at a multiplicity of infection (MOI) between 20 to 50 and plates incubated for
378 45 to 60 min to allow for uptake of bacteria. Cells were then washed three times with PBS and
379 fresh culture medium containing 50 μg/ml gentamicin was added to each well to kill extracellular
380 bacteria. After 2 hours the concentration of gentamicin was reduced to 5 μg/ml. At selected time
381 points gentamicin was removed by PBS washes and bacteria were recovered by lysis of
382 mammalian cells in sterile water with 0.1% Triton X-100. Lysates were serially diluted in PBS
383 and the bacteria were enumerated on LB agar plates.

384 ROS detection. 3×10^5 PEM were seeded in 96-well opaque white plates in 200 μl of phenol red-
385 free IMDM, 10% FBS and primed for 14 hours with murine IFN-γ (Biolegend) at a final
386 concentration of 50 ng/ml. Alternatively, 3×10^5 neutrophils were seeded in KRPG buffer (145
387 mM NaCl, 4.86 mM KCl, 5.7 mM sodium phosphate, 0.54 mM CaCl₂, 1.22 mM MgSO₄, 5.5 mM
388 Glucose, pH 7.35). For ROS production in neutrophils, cells were incubated with 1 mM luminol
389 (Sigma) for 3 min. before adding phorbol myristate acetate (PMA)(InvivoGen) or
390 lipopolysaccharides (LPS) (InvivoGen) to a final concentration of 100 ng/ml. Luminescence was
391 read in an EnVision (PerkinElmer) plate reader. Some wells were treated with 10 nM
392 diphenyleneiodonium chloride (DPI) (Sigma) –a NADPH oxidase inhibitor– for 30 min prior to
393 addition of luminol. The same procedures were used with macrophages except the luminol
394 enhancer Diogenes (National Diagnostics) was also used (Yamazaki et al., 2011).

395 Recovery of phagocytosed bacteria and immunodetection. *S. typhimurium* strain GPM2014 /
396 pTrc99aSodCII3flag was cultured aerobically overnight in LB with ampicillin at 37°C. The bacteria
397 were pelleted, washed with sterile PBS and aliquots of the inoculum were frozen at -80 °C for
398 later analysis. Aliquots of the inoculum were also used to infect wild-type and Perforin-2 -/- PEMs
399 at a multiplicity of infection of about 20-50. After 1 hour incubation, the cells were washed three
400 times with PBS then IMDM with 10% FBS and 50 μg/ml gentamicin was added to each well. This
401 initial addition of gentamicin marked the 0 hour time point. After 2 hours the concentration of
402 gentamicin was decreased to 5 μg/ml. After 16 hours the cells were washed with PBS three
403 times, then PBS, 0.1% Triton-X 100 containing a proteinase inhibitor cocktail (Roche, Basel,
404 Switzerland) was added to each well. After a 5 min. incubation at 37°C the cells were manually
405 detached with a cell scraper, the bacterial cells were harvested by centrifuged at 4°C at 10, 000 g
406 × 10 min, and the supernatant was removed. Recovered phagocytosed bacteria (approximate 10⁶
407 CFU) and bacteria from the original LB culture were boiled in Laemmli loading buffer for 7 min.
408 The same infection procedure was conducted with wild-type and Perforin-2 -/- BMDMs except the
409 phagocytosed bacteria were collected at 1, 3 and 6 hours. The protein samples were separated
410 on 4-20% gradient SDS-PAGE gels and transferred to nitrocellulose membranes. The
411 membranes were blocked with 5% non-fat milk in Tris buffered saline containing 0.1% Tween-20
412 (TBST) for 2 hours and then incubated at 4°C for 16 hours with primary antibodies anti-FliC
413 (1:1000, Invivogen), anti-Flag (1:5000, Sigma) or anti-DnaK (1:5000, Abcam) diluted in TBST
414 with 5% non-fat milk. After three washes with TBST the membranes were incubated at 37°C for 1
415 hour with anti-mouse horseradish peroxidase-labeled secondary antibody (Jackson
416 ImmunoResearch Laboratories, West Grove, PA, USA) diluted 1:5000 in TBST with 5% non-fat
417 milk. An Odyssey FC Imaging System (LI-COR, Lincoln, NE, United States) was used to detect
418 and quantify chemiluminescence after addition of SuperSignal West Pico Chemiluminescent
419 Substrate (Thermo Fisher Scientific).

420 Murine infections. Bacteria were cultured overnight in LB medium at 37°C and diluted in sterile
421 PBS. For competition assays selected strains of *S. typhimurium* were mixed at a 1:1 ratio.
422 Perforin-2 +/+ and -/- 129X1/SvJ mice were inoculated by intraperitoneal (i.p.) injection. The CFU
423 of each inoculum was quantified by plating and ranged from 500 to 1,000 total CFUs. Spleens
424 and livers were collected four days after inoculation, and then homogenized (Omni International)
425 in 500 μ l PBST (PBS, 0.1% Tween-20). Homogenates were diluted in sterile PBS and plated in
426 triplicate on LB agar with antibiotic selection as appropriate for each strain in the initial inoculum.
427 For each spleen and liver, mean CFUs were used to calculate competitive indices (CI) according
428 to the following formula: $CI = (\text{strain A recovered} / \text{strain B recovered}) / (\text{strain A inoculum} / \text{strain}$
429 $\text{B inoculum})$.

430 Statistical analysis. Statistical analysis was performed with GraphPad Prism 7 software. Data
431 represent the mean \pm standard deviation (SD). Statistical difference was determined by the
432 Student's *t*-test. *P* values ≤ 0.05 were considered statistically significant. The number of
433 independent experimental replicates is indicated by *n*.

434

435 Table 1 Bacteria strains and plasmids

Strain	Description	Reference
LT2	Wild-type <i>S. Typhimurium</i>	(Nikaido et al., 1967)
LT2b	LT2 derivative that spontaneously lost pSLT virulence plasmid	this study
GPM2004	LT2 <i>attB</i> _λ ::pCAH63, chloramphenicol resistant	this study
GPM2004b	LT2b <i>attB</i> _λ ::pCAH63, chloramphenicol resistant	this study
ST188	LT2 Δ <i>sodCI</i> :: <i>kan</i>	this study
ST188b	LT2b Δ <i>sodCI</i> :: <i>kan</i>	this study
ST189	LT2 Δ <i>sodCI</i> Δ <i>sodCII</i> :: <i>kan</i>	this study
GPM2008	LT2 Δ <i>sodCI</i> Δ <i>sodCII</i> :: <i>kan attB</i> _λ ::pAH63Tc-sodCII	this study
GPM2014	LT2 pTrc99aSodCII3flag	this study

436

437

438

439 Table 2 Oligonucleotide Primers

Primer	Sequence ^a (5'–3')
sodCI-P1	<u>TACACAATATTGTCGCTGGTAGCTGGTGCCTCATCAGTTGT</u> GTAGGCTGGAGCTGCTTC
sodCI-P2	<u>ATTGTCACCGCCTTTATGGATCATCAATGAGTGACCTTTCAT</u> ATGAATATCCTCCTTAGT
sodCI-MfeI	<u>TTTCAATTG</u> ATTAATGGTATTTACGATACAACC
sodCI-HindIII	<u>TTTAAGCTT</u> ATGGCTATGTTGCTGTTATTTCTC
sodCII-P1	<u>GCAGGCCGCCAGCGAGAAAGTAGAGATGAATCTGGTGACT</u> GTGTAGGCTGGAGCTGCTTC
sodCII-P2	<u>CGCCGCCGCCGAGCGGTTTCGGCTGATCGGACATGTTATCA</u> TATGAATATCCTCCTTAGT
sodCII-EcoRI	<u>TTTGAATTCAACAGGCGACCACATGTAACGGAG</u>
sodCII-HindIII	<u>TTTAAGCTTCACTGGCTCCGGGTTATTTAATGA</u>
sodCII-1238	<u>GCGTCTAGAGGGT</u> TATGACGTGCCGTAATC
sodCII-1239	<u>GCGGGATCCTCTTCACTTGTTCGTCATCGTCCTTGTAGTCTTT</u> AATGACGCCGCAGGCGTAAC
sodCII-1329	<u>ACCCGGGGATCCTTT</u> ATGACGTGCCGTAATCGC
sodCII-1330	<u>TGTAGTCGAATTCTTTA</u> ATGACGCCGCAGGCGTAA
3flag-1331	<u>CGGCGTCATTAAAGA</u> ATTCGACTACAAAGACCATGACG
3flag-1332	<u>CAAACAGCCAAGGGA</u> ACTTCGAAGCAGCTCCAG
pTrc99a-1333	<u>GCTTCGAAGTTCCCTT</u> GGCTGTTTTGGCGGATGA
pTrc99a-1334	<u>CGGCACGTCATAAAGGATCCCCGGGT</u> ACCGAG

440 ^aUnderlined nucleotides indicate primer/template mismatches.

441

442

443

444

445

446 **Acknowledgments**

447 Research reported in this publication was supported by Grant Number AI110810 from the
448 National Institute of Allergy and Infectious Diseases of the National Institutes of Health (NIAID
449 NIH). Its contents are solely the responsibility of the authors and do not necessarily represent the
450 official views of the NIH.

451 **Author Contributions**

452 Conceptualization, F.B., R.M.M., M.G.L., and G.P.M.; Methodology, F.B., R.M.M., and G.P.M.;
453 Investigation, F.B.; Validation, F.B. and G.P.M.; Formal Analysis, F.B.; Resources, S.H., G.V.P.,
454 and R.M.M.; Writing – Original Draft, F.B. and G.P.M.; Writing – Review & Editing, F.B., R.M.M.,
455 S.H., G.V.P., M.G.L., and G.P.M.; Visualization, F.B. and G.P.M.; Supervision, M.G.L. and
456 G.P.M.; Funding Acquisition, G.P.M.

457 **Declaration of Interests**

458 The authors declare no competing interests.

459

460 **References**

- 461 Amann, E., Ochs, B., and Abel, K.J. (1988). Tightly regulated tac promoter vectors useful for the
462 expression of unfused and fused proteins in *Escherichia coli*. *Gene* *69*, 301-315.
- 463 Anderson, C.J., and Kendall, M.M. (2017). *Salmonella enterica* Serovar Typhimurium Strategies
464 for Host Adaptation. *Frontiers in microbiology* *8*, 1983.
- 465 Aussel, L., Zhao, W., Hebrard, M., Guilhon, A.A., Viala, J.P., Henri, S., Chasson, L., Gorvel, J.P.,
466 Barras, F., and Meresse, S. (2011). *Salmonella* detoxifying enzymes are sufficient to cope with
467 the host oxidative burst. *Molecular microbiology* *80*, 628-640.
- 468 Benard, E.L., Racz, P.I., Rougeot, J., Nezhinsky, A.E., Verbeek, F.J., Spink, H.P., and Meijer,
469 A.H. (2015). Macrophage-expressed perforins mpeg1 and mpeg1.2 have an anti-bacterial
470 function in zebrafish. *Journal of innate immunity* *7*, 136-152.
- 471 Cederlund, A., Gudmundsson, G.H., and Agerberth, B. (2011). Antimicrobial peptides important in
472 innate immunity. *The FEBS journal* *278*, 3942-3951.
- 473 Craig, M., and Slauch, J.M. (2009). Phagocytic superoxide specifically damages an
474 extracytoplasmic target to inhibit or kill *Salmonella*. *PloS one* *4*, e4975.
- 475 Datsenko, K.A., and Wanner, B.L. (2000). One-step inactivation of chromosomal genes in
476 *Escherichia coli* K-12 using PCR products. *Proceedings of the National Academy of Sciences of*
477 *the United States of America* *97*, 6640-6645.
- 478 Duclos, S., Clavarino, G., Rousserie, G., Goyette, G., Boulais, J., Camossetto, V., Gatti, E.,
479 LaBoissiere, S., Pierre, P., and Desjardins, M. (2011). The endosomal proteome of macrophage
480 and dendritic cells. *Proteomics* *11*, 854-864.

- 481 Dudkina, N.V., Spicer, B.A., Reboul, C.F., Conroy, P.J., Lukoyanova, N., Elmlund, H., Law, R.H.,
482 Ekkel, S.M., Kondos, S.C., Goode, R.J., *et al.* (2016). Structure of the poly-C9 component of the
483 complement membrane attack complex. *Nature communications* 7, 10588.
- 484 Ellison, R.T., 3rd, and Giehl, T.J. (1991). Killing of gram-negative bacteria by lactoferrin and
485 lysozyme. *The Journal of clinical investigation* 88, 1080-1091.
- 486 Fang, F.C., DeGroot, M.A., Foster, J.W., Baumler, A.J., Ochsner, U., Testerman, T., Bearson,
487 S., Giard, J.C., Xu, Y., Campbell, G., and Laessig, T. (1999). Virulent *Salmonella typhimurium*
488 has two periplasmic Cu, Zn-superoxide dismutases. *Proceedings of the National Academy of*
489 *Sciences of the United States of America* 96, 7502-7507.
- 490 Fields, K.A., McCormack, R., de Armas, L.R., and Podack, E.R. (2013). Perforin-2 restricts
491 growth of *Chlamydia trachomatis* in macrophages. *Infection and immunity* 81, 3045-3054.
- 492 Gallo, R.L., Kim, K.J., Bernfield, M., Kozak, C.A., Zanetti, M., Merluzzi, L., and Gennaro, R.
493 (1997). Identification of CRAMP, a cathelin-related antimicrobial peptide expressed in the
494 embryonic and adult mouse. *The Journal of biological chemistry* 272, 13088-13093.
- 495 Gudmundsson, G.H., Agerberth, B., Odeberg, J., Bergman, T., Olsson, B., and Salcedo, R.
496 (1996). The human gene FALL39 and processing of the cathelin precursor to the antibacterial
497 peptide LL-37 in granulocytes. *European journal of biochemistry* 238, 325-332.
- 498 Haldimann, A., and Wanner, B.L. (2001). Conditional-replication, integration, excision, and
499 retrieval plasmid-host systems for gene structure-function studies of bacteria. *Journal of*
500 *bacteriology* 183, 6384-6393.
- 501 Hebrard, M., Viala, J.P., Meresse, S., Barras, F., and Aussel, L. (2009). Redundant hydrogen
502 peroxide scavengers contribute to *Salmonella* virulence and oxidative stress resistance. *Journal*
503 *of bacteriology* 191, 4605-4614.
- 504 Henzler Wildman, K.A., Lee, D.K., and Ramamoorthy, A. (2003). Mechanism of lipid bilayer
505 disruption by the human antimicrobial peptide, LL-37. *Biochemistry* 42, 6545-6558.
- 506 Karimi, G., Houee Levin, C., Dagher, M.C., Baciou, L., and Bizouarn, T. (2014). Assembly of
507 phagocyte NADPH oxidase: A concerted binding process? *Biochimica et biophysica acta* 1840,
508 3277-3283.
- 509 Kim, B., Richards, S.M., Gunn, J.S., and Slauch, J.M. (2010). Protecting against antimicrobial
510 effectors in the phagosome allows SodCII to contribute to virulence in *Salmonella enterica*
511 serovar Typhimurium. *Journal of bacteriology* 192, 2140-2149.
- 512 Krishnakumar, R., Craig, M., Imlay, J.A., and Slauch, J.M. (2004). Differences in enzymatic
513 properties allow SodCI but not SodCII to contribute to virulence in *Salmonella enterica* serovar
514 Typhimurium strain 14028. *Journal of bacteriology* 186, 5230-5238.
- 515 Krishnakumar, R., Kim, B., Mollo, E.A., Imlay, J.A., and Slauch, J.M. (2007). Structural properties
516 of periplasmic SodCI that correlate with virulence in *Salmonella enterica* serovar Typhimurium.
517 *Journal of bacteriology* 189, 4343-4352.

- 518 Laroux, F.S., Romero, X., Wetzler, L., Engel, P., and Terhorst, C. (2005). Cutting edge: MyD88
519 controls phagocyte NADPH oxidase function and killing of gram-negative bacteria. *Journal of*
520 *immunology* *175*, 5596-5600.
- 521 Law, R.H., Lukoyanova, N., Voskoboinik, I., Caradoc-Davies, T.T., Baran, K., Dunstone, M.A.,
522 D'Angelo, M.E., Orlova, E.V., Coulibaly, F., Verschoor, S., *et al.* (2010). The structural basis for
523 membrane binding and pore formation by lymphocyte perforin. *Nature* *468*, 447-451.
- 524 Lichtenheld, M.G., Olsen, K.J., Lu, P., Lowrey, D.M., Hameed, A., Hengartner, H., and Podack,
525 E.R. (1988). Structure and function of human perforin. *Nature* *335*, 448-451.
- 526 Luo, Y., and Dorf, M.E. (2001). Isolation of mouse neutrophils. *Current protocols in immunology*
527 *Chapter 3*, Unit 3 20.
- 528 Lutwyche, P., Cordeiro, C., Wiseman, D.J., St-Louis, M., Uh, M., Hope, M.J., Webb, M.S., and
529 Finlay, B.B. (1998). Intracellular delivery and antibacterial activity of gentamicin encapsulated in
530 pH-sensitive liposomes. *Antimicrobial agents and chemotherapy* *42*, 2511-2520.
- 531 Martinez, R.J., and Carroll, S.F. (1980). Sequential metabolic expressions of the lethal process in
532 human serum-treated *Escherichia coli*: role of lysozyme. *Infection and immunity* *28*, 735-745.
- 533 McClelland, M., Sanderson, K.E., Spieth, J., Clifton, S.W., Latreille, P., Courtney, L., Porwollik, S.,
534 Ali, J., Dante, M., Du, F., *et al.* (2001). Complete genome sequence of *Salmonella enterica*
535 serovar Typhimurium LT2. *Nature* *413*, 852-856.
- 536 McCormack, R., Bahnan, W., Shrestha, N., Boucher, J., Barreto, M., Barrera, C.M., Dauer, E.A.,
537 Freitag, N.E., Khan, W.N., Podack, E.R., and Schesser, K. (2016). Perforin-2 Protects Host Cells
538 and Mice by Restricting the Vacuole to Cytosol Transitioning of a Bacterial Pathogen. *Infection*
539 *and immunity* *84*, 1083-1091.
- 540 McCormack, R., de Armas, L.R., Shiratsuchi, M., Ramos, J.E., and Podack, E.R. (2013).
541 Inhibition of intracellular bacterial replication in fibroblasts is dependent on the perforin-like protein
542 (perforin-2) encoded by macrophage-expressed gene 1. *Journal of innate immunity* *5*, 185-194.
- 543 McCormack, R., and Podack, E.R. (2015). Perforin-2/Mpeg1 and other pore-forming proteins
544 throughout evolution. *Journal of leukocyte biology* *98*, 761-768.
- 545 McCormack, R.M., de Armas, L.R., Shiratsuchi, M., Fiorentino, D.G., Olsson, M.L., Lichtenheld,
546 M.G., Morales, A., Lyapichev, K., Gonzalez, L.E., Strbo, N., *et al.* (2015a). Perforin-2 is essential
547 for intracellular defense of parenchymal cells and phagocytes against pathogenic bacteria. *eLife*
548 *4*.
- 549 McCormack, R.M., Lyapichev, K., Olsson, M.L., Podack, E.R., and Munson, G.P. (2015b). Enteric
550 pathogens deploy cell cycle inhibiting factors to block the bactericidal activity of Perforin-2. *eLife*
551 *4*.
- 552 Nakamura, N., Lill, J.R., Phung, Q., Jiang, Z., Bakalarski, C., de Maziere, A., Klumperman, J.,
553 Schlatter, M., Delamarre, L., and Mellman, I. (2014). Endosomes are specialized platforms for
554 bacterial sensing and NOD2 signalling. *Nature* *509*, 240-244.

- 555 Nathan, C.F., and Root, R.K. (1977). Hydrogen peroxide release from mouse peritoneal
556 macrophages: dependence on sequential activation and triggering. *The Journal of experimental*
557 *medicine* *146*, 1648-1662.
- 558 Nauseef, W.M. (2004). Assembly of the phagocyte NADPH oxidase. *Histochemistry and cell*
559 *biology* *122*, 277-291.
- 560 Ni, T., and Gilbert, R.J.C. (2017). Repurposing a pore: highly conserved perforin-like proteins with
561 alternative mechanisms. *Philos Trans R Soc Lond B Biol Sci* *372*.
- 562 Nikaido, H., Levinthal, M., Nikaido, K., and Nakane, K. (1967). Extended deletions in the histidine-
563 rough-B region of the Salmonella chromosome. *Proceedings of the National Academy of*
564 *Sciences of the United States of America* *57*, 1825-1832.
- 565 Panday, A., Sahoo, M.K., Osorio, D., and Batra, S. (2015). NADPH oxidases: an overview from
566 structure to innate immunity-associated pathologies. *Cellular & molecular immunology* *12*, 5-23.
- 567 Podack, E.R., and Munson, G.P. (2016). Killing of Microbes and Cancer by the Immune System
568 with Three Mammalian Pore-Forming Killer Proteins. *Frontiers in immunology* *7*, 464.
- 569 Podack, E.R., Olsen, K.J., Lowrey, D.M., and Lichtenheld, M. (1989). Structure and function of
570 perforin. *Curr Top Microbiol Immunol* *140*, 11-17.
- 571 Podack, E.R., Tschoop, J., and Muller-Eberhard, H.J. (1982). Molecular organization of C9 within
572 the membrane attack complex of complement. Induction of circular C9 polymerization by the C5b-
573 8 assembly. *The Journal of experimental medicine* *156*, 268-282.
- 574 Podack, E.R., and Tschopp, J. (1982). Polymerization of the ninth component of complement
575 (C9): formation of poly(C9) with a tubular ultrastructure resembling the membrane attack complex
576 of complement. *Proceedings of the National Academy of Sciences of the United States of*
577 *America* *79*, 574-578.
- 578 Rosenberger, C.M., Gallo, R.L., and Finlay, B.B. (2004). Interplay between antibacterial effectors:
579 a macrophage antimicrobial peptide impairs intracellular Salmonella replication. *Proceedings of*
580 *the National Academy of Sciences of the United States of America* *101*, 2422-2427.
- 581 Slauch, J.M. (2011). How does the oxidative burst of macrophages kill bacteria? Still an open
582 question. *Molecular microbiology* *80*, 580-583.
- 583 Sonawane, A., Santos, J.C., Mishra, B.B., Jena, P., Progida, C., Sorensen, O.E., Gallo, R.,
584 Appelberg, R., and Griffiths, G. (2011). Cathelicidin is involved in the intracellular killing of
585 mycobacteria in macrophages. *Cellular microbiology* *13*, 1601-1617.
- 586 Spillsbury, K., O'Mara, M.A., Wu, W.M., Rowe, P.B., Symonds, G., and Takayama, Y. (1995).
587 Isolation of a novel macrophage-specific gene by differential cDNA analysis. *Blood* *85*, 1620-
588 1629.
- 589 Steele-Mortimer, O. (2008). The Salmonella-containing vacuole: moving with the times. *Current*
590 *opinion in microbiology* *11*, 38-45.

- 591 Stephan, A., Batinica, M., Steiger, J., Hartmann, P., Zaucke, F., Bloch, W., and Fabri, M. (2016).
592 LL37:DNA complexes provide antimicrobial activity against intracellular bacteria in human
593 macrophages. *Immunology* *148*, 420-432.
- 594 Storz, G., and Imlay, J.A. (1999). Oxidative stress. *Current opinion in microbiology* *2*, 188-194.
- 595 Thiery, J., Keefe, D., Boulant, S., Boucrot, E., Walch, M., Martinvalet, D., Goping, I.S., Bleackley,
596 R.C., Kirchhausen, T., and Lieberman, J. (2011). Perforin pores in the endosomal membrane
597 trigger the release of endocytosed granzyme B into the cytosol of target cells. *Nat Immunol* *12*,
598 770-777.
- 599 Tschopp, J., and Podack, E.R. (1981). Membranolysis by the ninth component of human
600 complement. *Biochemical and biophysical research communications* *100*, 1409-1414.
- 601 Turner, J., Cho, Y., Dinh, N.N., Waring, A.J., and Lehrer, R.I. (1998). Activities of LL-37, a
602 cathelin-associated antimicrobial peptide of human neutrophils. *Antimicrobial agents and*
603 *chemotherapy* *42*, 2206-2214.
- 604 Uzzau, S., Figueroa-Bossi, N., Rubino, S., and Bossi, L. (2001). Epitope tagging of chromosomal
605 genes in Salmonella. *Proceedings of the National Academy of Sciences of the United States of*
606 *America* *98*, 15264-15269.
- 607 Voskoboinik, I., Whisstock, J.C., and Trapani, J.A. (2015). Perforin and granzymes: function,
608 dysfunction and human pathology. *Nat Rev Immunol* *15*, 388-400.
- 609 Wiesner, J., and Vilcinskas, A. (2010). Antimicrobial peptides: the ancient arm of the human
610 immune system. *Virulence* *1*, 440-464.
- 611 Yamazaki, T., Kawai, C., Yamauchi, A., and Kuribayashi, F. (2011). A highly sensitive
612 chemiluminescence assay for superoxide detection and chronic granulomatous disease
613 diagnosis. *Tropical medicine and health* *39*, 41-45.
- 614 Zanetti, M. (2004). Cathelicidins, multifunctional peptides of the innate immunity. *Journal of*
615 *leukocyte biology* *75*, 39-48.
- 616 Zhang, X., Goncalves, R., and Mosser, D.M. (2008). The isolation and characterization of murine
617 macrophages. *Current protocols in immunology* *Chapter 14*, Unit 14 11.
- 618